SMiRT-12 / K. Kussmaul (Editor)
© 1993 Elsevier Science Publishers B.V. All rights reserved.

CRACK GROWTH ASSESSMENT FOR A CS-SPECIMEN COMPOSED OF RPV BASE AND CLADDING MATERIALS

A. Saarenheimo[1], H. Talja[1], H. Kordisch[2], B. Voss[2] and G.E. Neubrech[3]

[1]Technical Research Centre of Finland (VTT), Espoo, Finland
[2]Fh-IWM, Freiburg, Germany
[3]Kernforschungszentrum Karlsruhe, Germany

ABSTRACT

This study presents a stable crack growth evaluation for a side-grooved, multimaterial CS-type specimen, which was detached from the inner surface of the HDR reactor pressure vessel. The specimen was composed of ferritic base material and two austenitic cladding material layers. The specimen was tested at the Fraunhofer Institut für Werkstoffmechanik, Freiburg, Germany, and revealed an extremely nonuniform stable crack growth distribution along crack front.

Elastic-plastic finite element analyses were carried out using the 85-version of the ADINA code. For crack growth simulation a separate subroutine package IWM-CRACK linked with ADINA was used. Additional J-integral calculations were carried out based on the ADINA results using the VTTVIRT code in order to study the path-dependence of J-integral.

The crack growth was controlled by J_r-curves. Actual measured data was available only for the base material and hypothetical J_r-curves were applied for the two cladding layers. The calculated maximum load is slightly higher than the maximum load measured in the test.

The crack growth was relatively well simulated in quality. The slight numerical discrepancies at some locations along the crack front are consistent with extreme local material brittleness, which was clearly underestimated by the assumed material properties.

1. THE CS-SPECIMEN, GEOMETRY AND MATERIALS

The geometry of the tested CS-specimen is presented in Fig. 1. The inner radius of the specimen is 27.0 mm and outer radius 52.6 mm, respectively. The depth of the artificial crack is 15.0 mm and the thickness of the specimen is 12.7 mm. The tested 20 % side-grooved CS-specimen consists of a base material and two layers of cladding as layers across the thickness of the specimen with different material properties. The thickness of the base material layer is 5.5 mm and cladding materials 3.2 mm and 4.0 mm, respectively. The inner cladding material is called "cladding (1)" and the outer one "cladding (2)".

The material parameters were measured through the wall thickness of the HDR reactor pressure vessel by means of flat tensile micro specimens. Measured stress values through the specimen thickness and ultimate strain and the strain corresponding to the maximum stress value are presented in Fig. 2, /1/. R_{p02} is the engineering 0.2 % yield stress and R_m is the engineering stress corresponding to the maximum force.

2. FINITE ELEMENT CALCULATIONS

Elastic-plastic finite element analyses were carried out using the 85-version of the ADINA code /2/. In crack growth analyses a separate subroutine package IWM-CRACK /3/ linked with ADINA was used. In the calculation the full Newton iteration process with a line search was adopted for the solution of equilibrium equations. Additional J-integral calculations were carried out based on the ADINA results using the VTTVIRT /4/ code.

The finite element model is presented in Fig. 3. Due to the symmetry, only one half of the specimen was modelled. Because the material properties vary asymmetrically through the specimen, the whole specimen thickness had to be considered. The model consists of 689 20-noded three dimensional elements with 2*2*2 integration. The number of degrees of freedom is 11592. During the calculation the prescribed displacement in the crack opening direction at point A in Fig. 3 was increased. The load-line displacements in the cross direction were forced by constraint equations to stay on the same line (point A). Bending effects due to differing material properties were allowed. There were three element layers for the base material, one of which was used to model the side grooved area. One element layer was needed to model the inner cladding (1) material. For the outer cladding (2) material two element layers were used. One of them described the side-groove. Both mixed transition layers between two different materials were modelled with one element layer.

Five different stress-strain curves were used in the calculations. There were one stress-strain curve for each material (base material and two cladding materials) and two additional stress-strain curves describing the material properties of the mixed transition layers. Material properties used in the calculations were evaluated from the measured values (Fig. 2) as averages. Piecewise linear stress-strain curves used in the calculations are presented in Fig. 4. An isotropic yield hardening material model with von Mises yield function was adopted. Only the material nonlinearities were taken into consideration.

J_r-curves used as crack growth criterias are shown in Fig. 5. Actually, measured J_r-curves were available only for the base material, but two different crack growth criterias were used as shown in Fig. 5. The lower J_r-curve is the measured curve for the base material. It was applied also for the cladding (1), which was thus assumed to have the same toughness as the base material. The cladding (2) material is much tougher than the other two materials. The fracture resistance curve for the cladding (2) material was obtained by multiplying the J_r-values for the base material by two.

2.1 J-integration paths

Materially nonlinear FE-calculation without crack growth was first carried out in order to study the numerical path-independence of the J-integrals calculated from different paths. This calculation was made using the ADINA and the VTTVIRT programs. The aim of this study is to help to choose relevant integration paths to control the crack growth along the crack front.

One step corresponding to load point displacement of 0.362 mm was calculated. J-integrals were evaluated from seven different paths J1, J6, J13, J16, J25, J33 and J43, which are shown in Fig. 6. The numbers (e.g. 43 in J43) indicate the number of nodal points defining each path. The J-integration paths defined by element corner nodes are located either at the interfaces between different materials or at the bottom of the side grooves. In both cases the J-integral calculation might be inaccurate. In the latter case this is due to the finite element modelling of the side groove.

J-integral values were calculated also from the mid-side nodes using paths J16, J25 and J33. They are presented in Fig. 7 together with the J-values calculated from corner nodes. In this case the integration areas consist of one element layer and thus one material only. The values obtained from corner and mid-side nodes agree quite well. The values at the bottom of the side grooves may be slightly too high because the finite element model causes an extra singularity in the through-the-specimen-thickness direction. In the following crack growth analysis the largest path J43 was chosen to control the crack growth. It is expected to yield the best path-independence of J during the crack growth.

2.2 Crack growth analysis

The prescribed displacement in the crack opening direction at point A (Fig. 3) was increased step by step (each step 0.05 mm) 21 times. At each step the calculated J-integral values were compared to the given J_r-curves, and the nodes at the ligament were shifted and released (sequentially releasing the constrained nodes adjacent the crack tip) according to the crack growth criterias, which are presented in Fig. 5. In this calculation nearly 10 hours of CPU-time in a Cray XMP-computer was needed.

To study the path-independence of J-integral during the crack growth, J-integrals were calculated from paths J16, J25, J33 and J43. They were calculated at the corner nodes for all element layers presented in chapter 2.

3. COMPARISON OF THE EXPERIMENTAL AND NUMERICAL RESULTS

The calculated and measured load-displacement curves are shown in Fig. 8. The calculated maximum load is about 16 % higher than the maximum load value measured in the test. The shapes of the measured and calculated curves agree quite well. It is apparent that the agreement between the experimental and the numerical simulation is not as good in the descending part of the displacement curve as in the ascending part. Reasons for this phenomena are the lack of proper J_r-curves for the cladding materials and uncertainties in the assumed stress-strain curves of different material layers.

The calculated J-integral values through the specimen thickness are presented in Fig. 9 at calculation steps N=5, N=10, N=15 and N=21 corresponding the load-line displacement values of .458 mm, .973 mm, 1.49 mm and 2.12 mm, respectively. The shape of the J-integral value distribution through the specimen remains quite the same until the crack starts to grow at the fifth load step.

The estimated crack growth at the end of the calculation and the measured crack growth values after the test are presented in Fig. 10. The measured crack growth is somewhat greater than the calculated. Especially this holds for the cladding (1), where the same crack growth resistance curve as in base material was applied. In the base material and in the cladding (2) material the agreement is quite satisfactory.

Fig. 2 shows that the cladding (1) is very brittle. Especially the transition zones adjacent to the base material and to cladding (2) are extremely unyielding. This is clearly underestimated by the assumed stress-strain curves and J_r-curves, see the bold arrows in Figs. 4 and 5. The calculated results should not be improved by playing with uncovered parameters. But there is no doubt that the tendencies indicated by the bold arrows in Figs. 4 and 5 are responsible for the underestimation of the calculated crack growth in cladding (1), see the bold arrow in Fig. 10. As a consequence of the calculated too small crack area, the calculated compliance of the specimen is likewise underestimated, compare the bold

arrow in Fig. 8.

The underestimation of the brittleness of the cladding (1) in this calculation was well-founded because the mentioned unyielding stress-strain curves were measured on original HDR-material taken from an area that had seen about 9,500 sharp thermal shocks. In contrast to this the specimen considered in this calculation was detached from an other RPV area that was not damaged by thermal shocks. Therefore the stress-strain curves had to be used with prudence. But the comparison of the experimental and numerical results indicates that the extreme brittleness of cladding (1) is due to fabrication and not thermal shock.

4. CONCLUSIONS

The crack growth was relatively well simulated in quality. The numerical discrepancies are consistent with the extreme local material brittleness clearly underestimated by the assumed material properties. With more accurate strength properties and measured crack-resistance curves more accurate crack growth results are thought to be reached. In that case also the calculated load-displacement curve might be somewhat closer to the measured graph.

REFERENCES

/1/ Guenes, Haubner, Opel. 1990. Bestimmung des Eigenspannung- und E-Modulverlaufes an der Innenwand des HDR-RDB. Siemens/KWU-Bericht E 113/90/39, 04/90 PHDR-Arbeitsbericht z. 349/90.

/2/ Bathe, K.-J. 1980. ADINA, a Finite Element Program for Automatic Dynamic Incremental Nonlinear Analysis. Report 82 448-1, MIT, Cambridge Mass., USA.

/3/ IWM-CRACK, a subroutine package for crack problems, Fraunhofer-Institut für Werkstoffmechanik, Freiburg, FRG.

/4/ Talja, H. 1987. Elastic-plastic fracture parameters and their calculation by finite element method. Espoo. 113p (in Finnish).

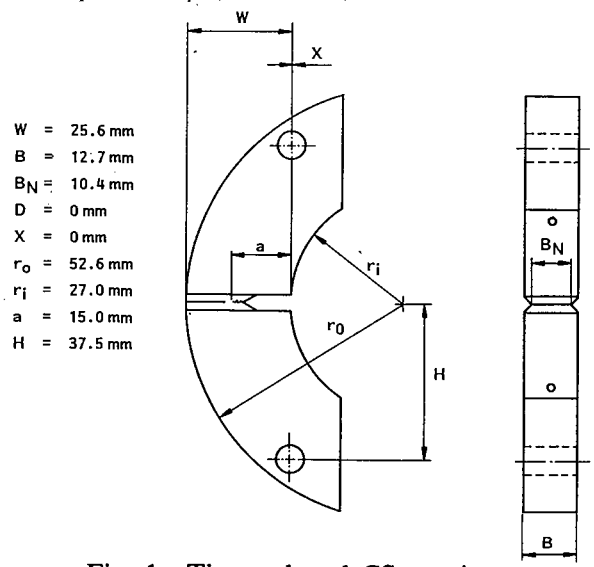

Fig. 1. The analyzed CS-specimen.

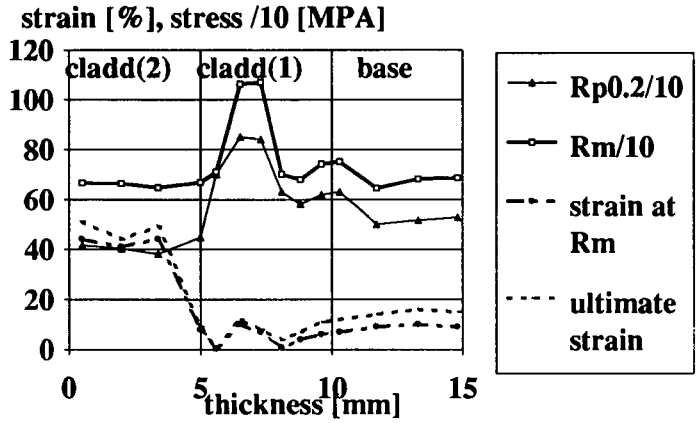

Fig. 2. Measured strength and strain values.

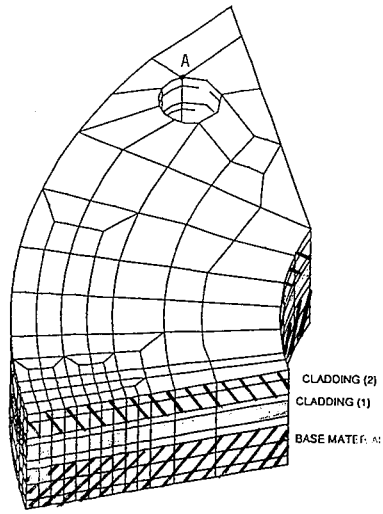

Fig. 3. Finite element model.

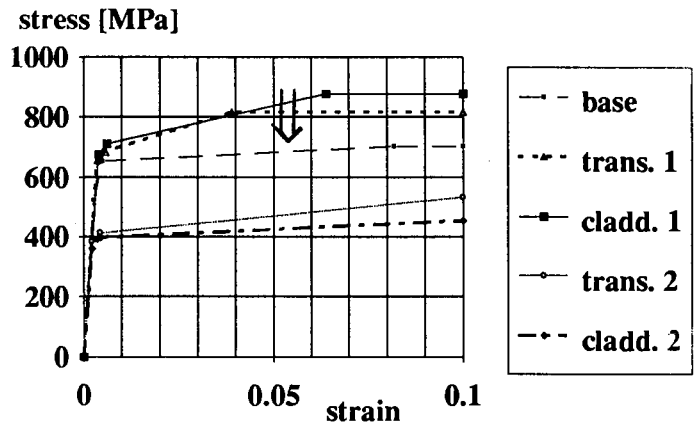

Fig. 4. Stress-strain curves.

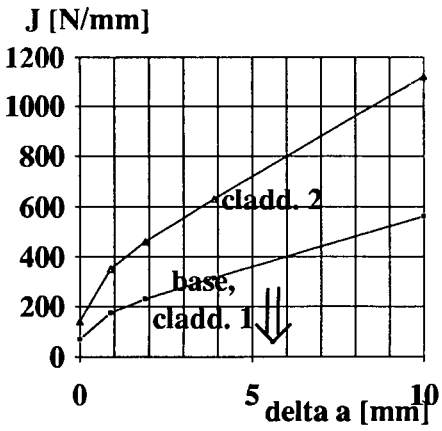

Fig. 5. J_R-curves.

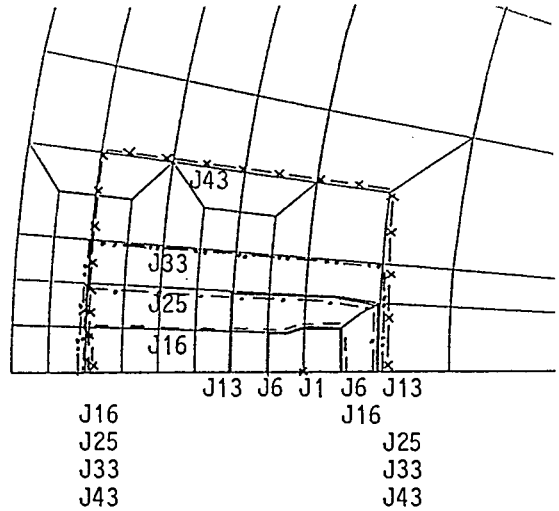

Fig. 6. J-integral paths.

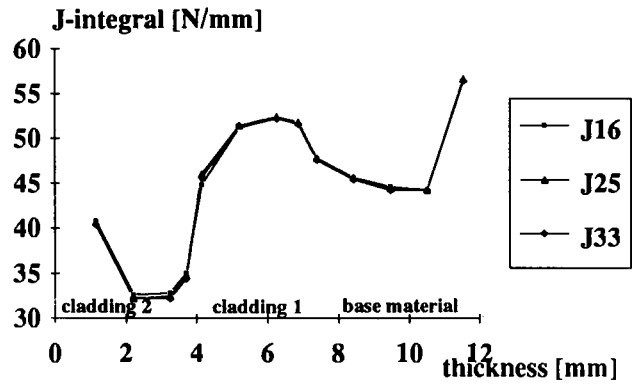

Fig. 7. J-integral values in corner and midside nodes.

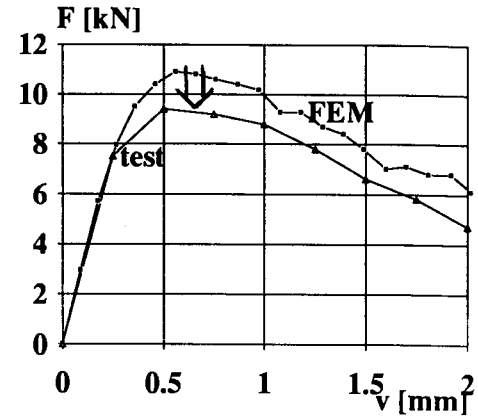

Fig. 8. Load-displacement curves.

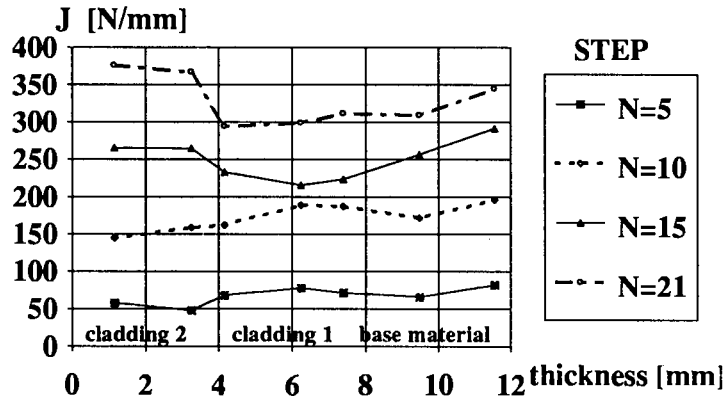

Fig. 9. Calculated J-integral values through the specimen thickness.

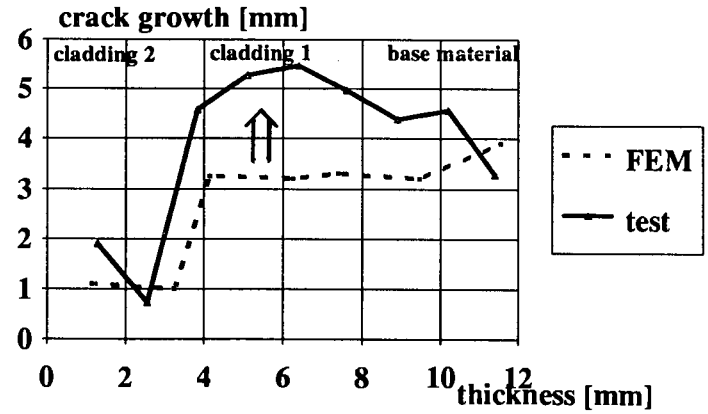

Fig. 10. Measured and calculated crack growth.